A large bandwidth photonic delay line using passive cascaded silicon-on-insulator microring resonators*

Hu Ying-Tao(胡应涛)[a], Xiao Xi(肖 希)[a], Li Zhi-Yong(李智勇)[a], Li Yun-Tao(李运涛)[a], Fan Zhong-Chao(樊中朝)[b], Han Wei-Hua(韩伟华)[b], Yu Yu-De(俞育德)[a], and Yu Jin-Zhong(余金中)[a]†

[a] *State Key Laboratory on Integrated Optoelectronics, Institute of Semiconductors, Chinese Academy of Sciences, Beijing* 100083, *China*

[b] *Engineering Research Center for Semiconductor Integrated Technology, Institute of Semiconductors, Chinese Academy of Sciences, Beijing* 100083, *China*

(Received 25 January 2011; revised manuscript received 27 February 2011)

This paper investigated the design and the characterization of a photonic delay line based on passive cascaded silicon-on-insulator (SOI) microrings. We considered the compromise of group delay, bandwidth and insertion loss. A 3-stage double channel side-coupled integrated spaced sequence of resonator (SCISSOR) device was optimized by shifting the resonance of each microring and fabricated with electron beam lithography and dry etching. The group delay was measured to be 17 ps for non-return-to-zero signals at different bit rates and the bandwidth of 78 GHz was achieved. The experiment result agreed well with our simulation.

Keywords: group delay, delay line, slow light, microring resonator

PACS: 42.60.Da, 42.79.–e, 42.82.–m **DOI:** 10.1088/1674-1056/20/7/074208

1. Introduction

Photonic delay lines are widely applied in data buffering, signal processing, quantum computing and phase controlling in phased array antenna.[1−4] Slow light has emerged as an enabling technology for slowing down the speed of light to achieve optical pulse delay. Among various approaches for optical pulse delays based on slow light, high-index-contrast microring resonator is considered as one of the most potential schemes owing to the compact size and the on-chip integration. For a single microring resonator, a large delay can be obtained by approaching the critical coupling within the over-coupled state.[5] But it suffers from the extreme limit of the transmission bandwidth and the difficulty in approaching the critical coupling point during the fabrication. Cascaded microring structure can enlarge the group delay and increase the bandwidth, which is regarded to be promising for on-chip optical delays. However, it's difficult to fabricate frequency-matched cascaded microrings because the response of high-index-contrast microring is very sensitive to the fabrication error and to the optical effect of coupling frequency shifts (CIFS).[6] In order to enlarge the bandwidth, large number of microrings and resonance tuning schemes, such as thermo-optic effect, have been explored to relax the fabrication requirement and to control the resonance location for frequency matching in the previous publications.[7−9] However, they lack for a comprehensive design of photonic delay line based on passive cascaded microring. This paper investigates the detailed design of photonic delay line based on the passive cascaded silicon on insulator (SOI) microring, considering the total group delay, the bandwidth, as well as the insertion loss. Experimentally, a large bandwidth photonic delay line based on 3-stage passive cascaded SOI microring resonators with good frequency matching is fabricated. The cascaded microring structure is configured with double-channel side-coupled integrated spaced sequence of resonators (SCISSOR).[10] It exhibits a group delay of 17 ps and a bandwidth of

*Project supported by the National Basic Research Program of China (Grant Nos. 2006CB302803 and 2011CB301701), the National Natural Science Foundation of China (Grant No. 60877036), State Key Laboratory of Advanced Optical Communication Systems and Networks of China (Grant No. 2008SH02), and the Knowledge Innovation Program of Institute of Semiconductors, Chinese Academy of Sciences (Grant No. ISCAS2008T10).

†Corresponding author. E-mail: jzyu@semi.ac.cn

© 2011 Chinese Physical Society and IOP Publishing Ltd

78 GHz at the through port.

2. Design of SCISSOR slow light delay lines

The double-channel SCISSOR consists of a series of add–drop microrings, which are connected with each other by the bus waveguides, as shown in Fig. 1. The transfer properties of a finite sequence of cascaded microrings can be obtained using the transfer matrix method.

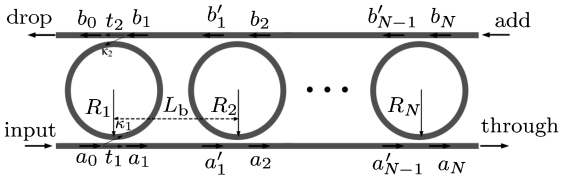


Fig. 1. The schematic diagram of the double-channel SCISSOR.

For a single add–drop microring, the incident field a_0 (b_1) and the transmitted field a_1 (b_0) at the coupling area can be related with the following transfer matrix:

$$\begin{pmatrix} a_1 \\ b_0 \end{pmatrix} = \begin{pmatrix} s_{11} & s_{12} \\ s_{21} & s_{22} \end{pmatrix} \begin{pmatrix} a_0 \\ b_1 \end{pmatrix}, \tag{1}$$

where

$$s_{11} = \frac{t_1 - at_2\,\mathrm{e}^{\mathrm{i}\,\phi}}{1 - at_1t_2\,\mathrm{e}^{\mathrm{i}\,\phi}}, \quad s_{22} = \frac{t_2 - at_1\,\mathrm{e}^{\mathrm{i}\,\phi}}{1 - at_1t_2\,\mathrm{e}^{\mathrm{i}\,\phi}},$$
$$s_{12} = s_{21} = -\frac{a\kappa_1\kappa_2\,\mathrm{e}^{\mathrm{i}\,\phi/2}}{1 - at_1t_2\,\mathrm{e}^{\mathrm{i}\,\phi}},$$

$t_{1,2}$ and $\kappa_{1,2}$ are the transmission and the coupling coefficients between the bus waveguide and the microring at the through and the drop sides, respectively, a represents the round-trip amplitude attenuation and $\phi = n_\mathrm{r} \cdot (2\pi/\lambda) \cdot 2\pi R$ is the round-trip phase shift in the ring. The above S-matrix can be converted to the following T-matrix for mathematical convenience:

$$\begin{pmatrix} a_1 \\ b_1 \end{pmatrix} = \begin{pmatrix} t_{11} & t_{12} \\ t_{21} & t_{22} \end{pmatrix} \begin{pmatrix} a_0 \\ b_0 \end{pmatrix}, \tag{2}$$

where $t_{11} = s_{11} - s_{12}s_{21}/s_{22}$, $t_{12} = s_{12}/s_{22}$, $t_{21} = -s_{21}/s_{22}$, $t_{22} = 1/s_{22}$.

The light propagation in the two waveguides connecting each two adjacent rings can also be described using a transfer matrix:

$$\begin{pmatrix} a'_1 \\ b'_1 \end{pmatrix} = \begin{pmatrix} \mathrm{e}^{-\eta+\mathrm{i}\,\phi_\mathrm{b}} & 0 \\ 0 & \mathrm{e}^{\eta-\mathrm{i}\,\phi_\mathrm{b}} \end{pmatrix} \begin{pmatrix} a_1 \\ b_1 \end{pmatrix}, \tag{3}$$

where η is the field loss in the waveguides connecting each two adjacent rings and $\phi_\mathrm{b} = n_\mathrm{b} \cdot (2\pi/\lambda) \cdot L_\mathrm{b}$ is the phase shift in the bus waveguide of length L_b.

Therefore, the transfer matrix relation of the first stage can be obtained from Eqs. (2) and (3),

$$\begin{pmatrix} a'_1 \\ b'_1 \end{pmatrix} = \begin{pmatrix} \mathrm{e}^{-\eta+\mathrm{i}\,\phi_\mathrm{b}}t_{11} & \mathrm{e}^{-\eta+\mathrm{i}\,\phi_\mathrm{b}}t_{12} \\ \mathrm{e}^{\eta-\mathrm{i}\,\phi_\mathrm{b}}t_{21} & \mathrm{e}^{\eta-\mathrm{i}\,\phi_\mathrm{b}}t_{22} \end{pmatrix} \begin{pmatrix} a_0 \\ b_0 \end{pmatrix}$$
$$\equiv T_1 \begin{pmatrix} a_0 \\ b_0 \end{pmatrix}. \tag{4}$$

Then, the transfer matrix of N-stage double-channel SCISSOR is obtained by multiplying transfer matrices of each unit

$$\begin{pmatrix} a'_N \\ b'_N \end{pmatrix} = T_1 \cdot T_2 \cdots T_N \begin{pmatrix} a_0 \\ b_0 \end{pmatrix}. \tag{5}$$

So the power transmission and the phase shift of the through port can be found from the total matrix as $T_\mathrm{thr} = |a'_N/a_0|^2$ and $\Phi_\mathrm{thr} = \arg(a'_N/a_0)$, respectively and the group delay time can be derived as $\tau_\mathrm{thr} = -\partial\Phi_\mathrm{thr}/\partial\omega$. Similarly, the results for the drop port can be obtained.

A single add–drop ring function as a slow light element when the over-coupling condition $t_1 < at_2$ is satisfied at the through port. It always generates a positive group delay at the drop port in any coupling condition.[5] Therefore, each ring of the double-channel SCISSOR should be over-coupled to make a delay line.

When multiple identical rings that have the same dimensions and the same coupling coefficients are cascaded, the resonances of each ring will locate at the same wavelength and the group delay will be enhanced as well as the bandwidth. However, the insertion loss of the cascaded structure is also increased. If a small resonance shift is introduced to each ring to make a spread for each individual resonance, the insertion loss will be reduced at the cost of a smaller total group delay. Meanwhile, the bandwidth will be much larger. It's a trade-off among the group delay, the bandwidth and the loss. Their relationship is illustrated in Fig. 2, in which the dot lines and the dash lines are the transmission and the group delay responses of the 1-stage ring and the 3-stage identical rings, respectively. Here, the radius of the rings is assumed to be around 10 μm with gradual variation, thus making uniform resonance spacing. The effective refractive index of the SOI ring waveguide is set as 2.91. The propagation loss of the SOI ring waveguide and the bus waveguide

are assumed to be 13.89 dB/cm and 4.14 dB/cm, respectively, with $a = 0.99$ and $e^{-\eta} = 0.9985$. The coupling coefficients are set as $t_1 = 0.945$ and $t_2 = 0.975$ at the through and the drop sides, respectively. The simulation results show that the maximal group delay is enhanced from 35.7 ps to 121.5 ps and the bandwidth increases from 0.109 nm to 0.125 nm. However the insertion loss also increases from 12.76 dB to 23.13 dB. When small differences are introduced to the dimensions of the microrings, so that the resonance wavelengths of individual microrings are distributed, the bandwidth is further broadened to 0.27 nm and the insertion loss is greatly decreased to 15.2 dB. In addition, the group delay (68.1 ps) is much larger than that of the 1-stage ring (35.7 ps). The solid line in Fig. 2 shows the transmission and the group delay responses of the design with resonance spacing of 0.1 nm. As the resonance spacing increases, the bandwidth can be further expanded, while the maximum group delay is reduced and much large ripples emerge in both the transmission and the group delay curves, as shown by the dot-dash lines in Fig. 2. As a result, a balance among the resonance spacing, the uniformity of the transmission and the group delay is necessary.

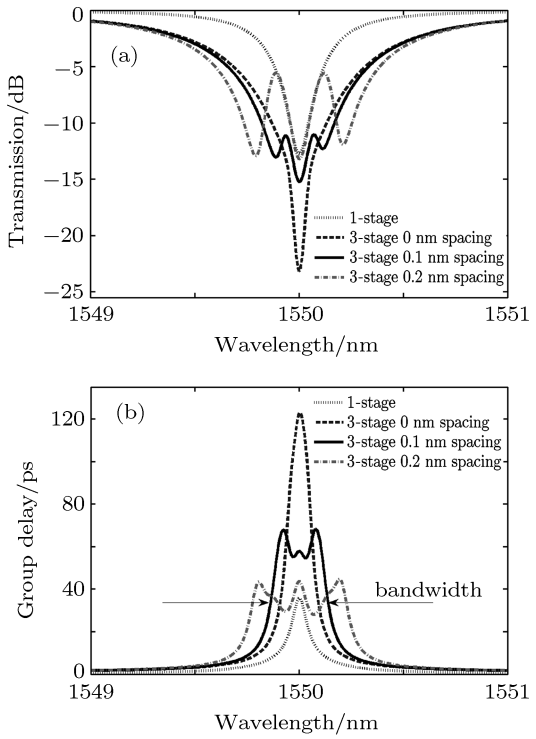


Fig. 2. (a) The transmission and (b) the group delay characteristics of 1-stage and 3-stage double-channel SCISSORs with: $R = 10$ μm, $t_1 = 0.945$, $t_2 = 0.975$, $a = 0.99$, $e^{-\eta} = 0.9985$ and resolution of 0.001 nm.

Figures 3(a)–3(c) show the maximal group delay, the bandwidth and the insertion loss when different resonance spacings are introduced. Obviously, the maximal group delay decreases monotonically with the resonance spacing. When the resonance spacing is too large, the maximal group delay falls to the 1-stage ring's level. Meanwhile, the ripple in the group delay tends to increase monotonically as the resonance spacing is increased, as seen in the inset of Fig. 3(a). As shown in Fig. 3(b), the bandwidth increases almost linearly with the increasing resonance spacing. However, when the ripple in the delay is larger than 50% of the maximal group delay, the bandwidth will also decrease by 3 dB. Figure 3(c) depicts the dependence of insertion loss on the resonance spacing.

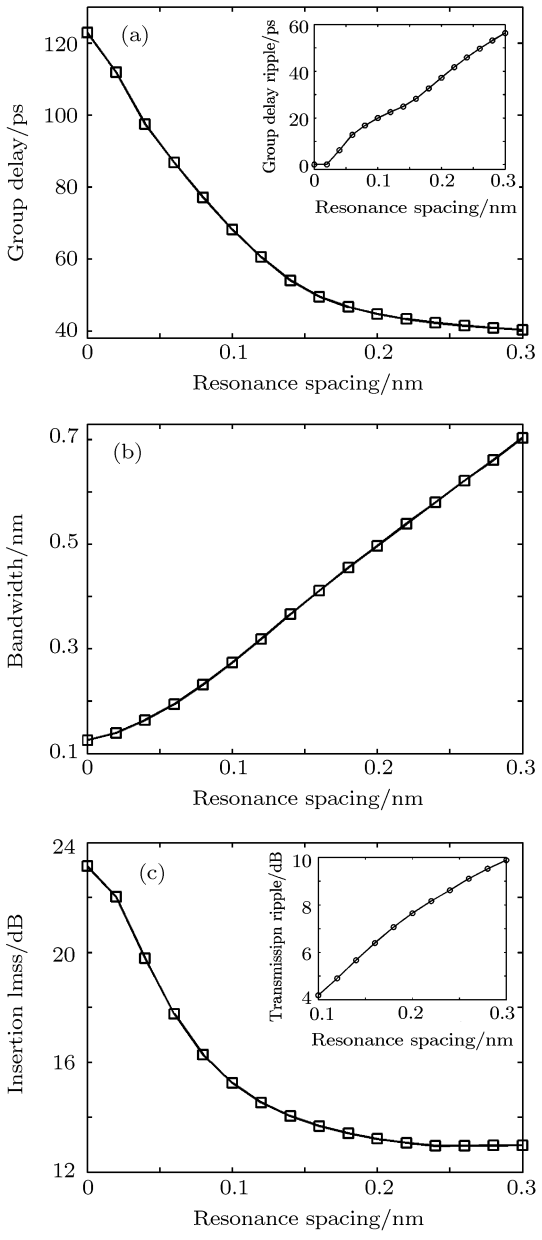


Fig. 3. Response curves of (a) maximal group delay, (b) bandwidth and(c) insertion loss when different resonance shifts are introduced.

If the resonance spacing is large enough, the insertion loss can be reduced to the 1-stage ring's level of about 12.76 dB, which can also be obtained from Fig. 2. The transmission ripple will not be negligible in such cases. In summary, the resonance spacing should not be too small to get the enlarged bandwidth and the decreased insertion loss; meanwhile, the resonance spacing should not be too large so that the group delay can be significantly enhanced and the ripples in the delay and in the transmission are negligible.

There is another type of resonances in the double-channel SCISSOR, the Bragg resonances, which occur at the Bragg wavelengths $\lambda_i = 2n_{\rm b}L_{\rm b}/i$ (i is an integer).[11] When the total phase shift in the bus waveguides between each two adjacent rings at the through and drop sides is matched with the round-trip phase shift in the ring, that is, the phase-matching condition $2n_{\rm b}L_{\rm b} = n_{\rm r} \cdot 2\pi R$ is satisfied, the microring resonances and the Bragg resonances will coincide with each other, thus the transmission bandwidth can be broadened.[12] In addition, the phase-matching design can be beneficial to making flat group delays in the bandwidth.

3. Device fabrication

The cascaded microring device was fabricated on a commercial SOI wafer with a top silicon thickness of 340 nm and a buried silica thickness of 2 μm. Electron beam lithography (EBL) and inductively-coupled-plasma (ICP) reactive ion etching were used to fabricate the device. At first, the electron-beam resist polymethyl–methacrylate (PMMA) was spun onto the wafer to create a masking layer. To improve the fiber-to-device light coupling, grating couplers[13] were integrated with the cascaded microrings by tapered waveguides conjoining. The whole device, which consists of waveguides, microrings and grating couplers, was defined with one step of electron beam lithography (Raith150). After developing of the resist, the device pattern was transferred into the PMMA mask. Then, the pattern was etched into the silicon layer by inductively-coupled-plasma (ICP) etching processes. A scanning electron microscopic (SEM) image of the fabricated cascaded microring structure is shown in Fig. 4. The radii of the microrings are 10 μm. The rib widths of the bus waveguide and the ring waveguide are 460 nm and 590 nm, respectively. The gaps between the bus waveguides and the ring waveguides are 180 ± 5 nm at the through and 190 ± 5 nm at the drop. The slab height is about 130 nm, which corresponds to a 210 nm etch depth.

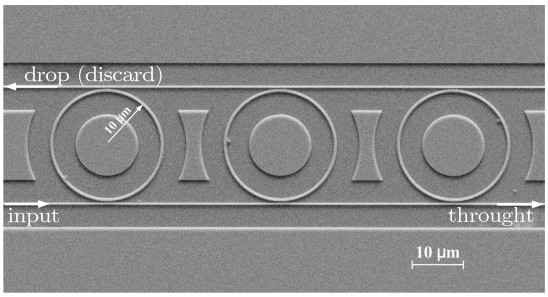


Fig. 4. SEM images of the 3-stage double-channel SCISSOR device.

4. Results and discussion

Fiber-to-fiber transmission measurements were carried out to characterize the spectral response of the cascaded microring devices. TE-polarized light from a tunable laser was coupled into the bus waveguide by using the grating couplers at the input port; and the light was coupled out of the device by using the grating coupler at the through port, which was then received by a flat-top optic fiber. The measured through-port response spectra of the 1-stage and the 3-stage double-channel SCISSOR devices are shown in Fig. 5. Clearly, the spectral bandwidth is broadened from 0.09 nm (corresponding to 11 GHz) of the 1-stage device to 0.627 nm (corresponding to 78 GHz) of the 3-stage device. And the insertion loss is increased from 12.5 dB to 22.0 dB. From the spectral parameters of the 1-stage microring, the major optical parameters of the single ring resonator can be extracted:[14] roundtrip attenuation factor, transmission and coupling coefficients are $a = 0.99$, $t_1 = 0.9449$, $t_2 = 0.9749$, $\kappa_1 = 0.3274$, $\kappa_2 = 0.2226$, respectively. These parameters completely describe the response of a resonator with a loaded Q of 3900, an intrinsic Q of 14000 and a group delay of 35.5 ps on resonance. Using these parameters and the 0.1 nm resonance spacing design, the maximal total group delay is 69.5 ps, which is obtained in a simulation of the 3-stage rings with a bandwidth of 0.27 nm (corresponding to 34 GHz).

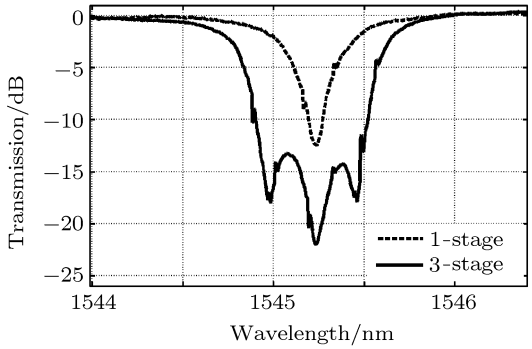


Fig. 5. Measured transmission spectra of 1- and 3-stage double channel SCISSOR devices.

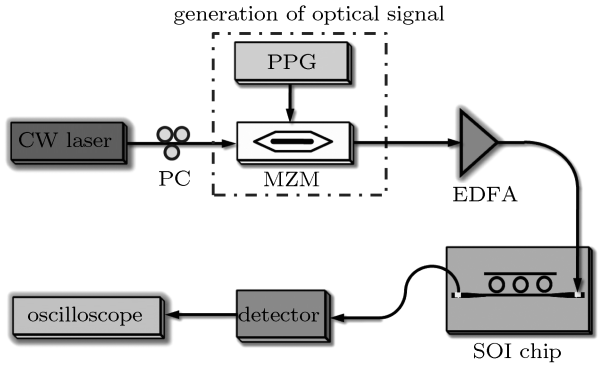


Fig. 6. Experimental setup. CW: continuous wave; PC: polarization controller; PPG: pulse pattern generator; MZM: Mach–Zehnder modulator.

Then, non-return-to-zero (NRZ) pseudo-random bit sequence (PRBS) signals at different bit rates were used to experimentally demonstrate the delay performance. The experimental setup is shown in Fig. 6. The signals was generated by a Mach–Zehnder modulator (MZM), which was driven by the PRBS signals of different bit rates from a pulse pattern generator (PPG) . The temporal response of the optical signal propagating through the double channel SCISSOR device was traced by an oscilloscope.

Figures 7(a)–7(e) demonstrates the measured results of the 3-stage double-channel SCISSOR for input signal bit rates of 1 Gbps, 3 Gbps, 5 Gbps, 10 Gbps and 12.5 Gbps, respectively. The solid curves are the pulse waveforms when the signal wavelengths are off-resonant with the ring; and the dash curves are the delayed pulse waveforms when the signal wavelengths are tuned on-resonant at the center of the transmission band (solid curve in Fig. 5). The group delay time at different bit rates is almost the same (about 17 ps as shown in Fig. 7(f)). Besides, the signal distortions of the delayed waveforms are negligible even at the highest measurement rate, which also is the limit of our equipments. This means that the bit rate does not reach the intrinsic bandwidth of the SCISSOR device. With the bandwidth of 78 GHz, a maximum allowable bit rate of 39 Gbps is expected.[7]

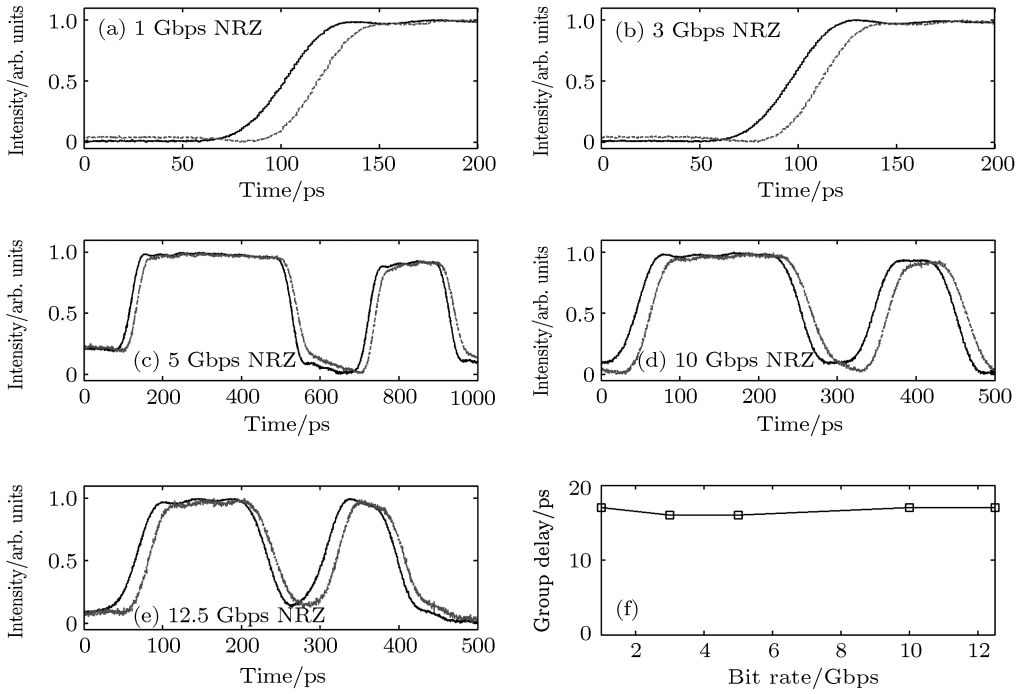


Fig. 7. (a)–(e) Measured group delay time of 3-stage double-channel SCISSOR device at different bit rates and (f) group delay time versus bit rate.

It should be noted that the measured group delays are much smaller than the simulated ones and the bandwidth is much larger than that in the simulations. According to the simulations in Section 2, the main reason should be that the actual resonance shift is much larger than the design value of 0.1 nm. In fact, according to the in-band ripples in the transmission spectrum, it can be found that the resonance shift is as large as 0.25 nm. The enlarged resonance shift may be resulted from the fabrication variations, including the deviations of the ring dimensions, of the gaps and of the width of the waveguides. By properly adjusting the optical parameters and the dimensions of the 3 cascaded microrings, a simulated spectrum for the through port fits well the measured spectrum, as shown in Fig. 8(a). In the simulation, the variations of the coupling coefficients are in the ranges of 0.3274 ± 0.073 and 0.2226 ± 0.046 at the through and the drop sides, respectively. The deviations of the microring radii are less than 1.6 nm. Then, using the

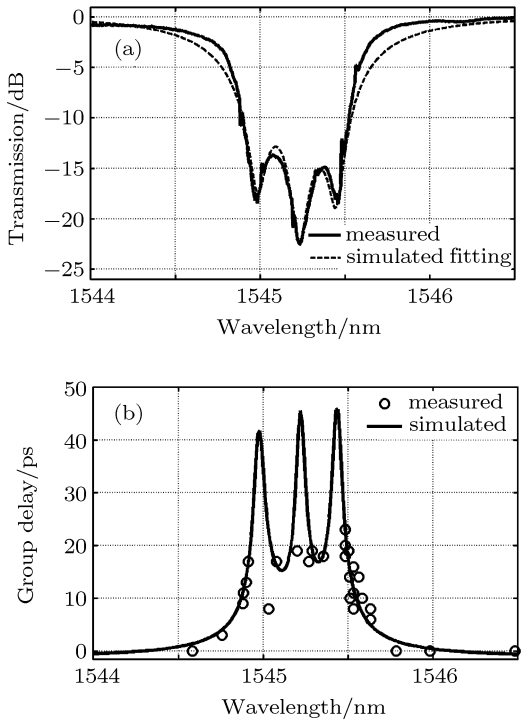


Fig. 8. (a) Measured and simulated transmissions and (b) the fitting to group delay.

adjusted optical parameters and the adjusted radii, the group delay versus the wavelength curve can be obtained, as shown in Fig. 8(b). The measured data of group delay are plotted with open circles in the figure. It is clear that a group delay of about 17 ps can be achieved in the whole bandwidth of about 78 GHz, which agrees well with the experimental results. The peak group delay can reach 45 ps, which is difficult to be observed in the measurements due to the narrow bandwidth and the light source fluctuation. The effect of group delay dispersion may also contribute to the minishing of the measured group delay. The ripples, which are as large as 20 ps and respond to the splits of several dB in the spectrum, are mainly caused by the overlarge resonance shift. So a fabrication with better accuracy, which means negligible splits and ripples, may result in better performance for the group delay.

5. Conclusion

This paper has systematically investigated an optical delay line based on passive SOI cascaded microrings. The performance was characterized for a 3-stage double-channel SCISSOR device, which exhibited good resonance matching, large bandwidth and enhanced group delay compared with a single microring. In experiment, the maximum delay of 17 ps at different bit rates and the bandwidth as large as 78 GHz were demonstrated. The performance of such a delay line can be further improved by increasing the number of cascaded microrings and by optimizing the resonance shifting and the coupling between the microrings and buses

Acknowledgement

The authors would like to thank Yang Fu-Hua and Ji An from the Engineering Research Center for Semiconductor Integrated Technology, Institute of semiconductors for their expert technical support.

References

[1] Fontaine NK, Yang J, Pan Z, Chu S, Chen W, Little BE and Ben Yoo S 2008 *J. Lightw. Technol.* **26** 3776
[2] Willner A, Zhang B, Zhang L, Yan L and Fazal I 2008 *IEEE J. Sel. Top. Quantum Electron.* **14** 691
[3] Julsgaard B, Sherson J, Cirac J, Fiuráek J and Polzik E 2004 *Nature* **432** 482
[4] Liu Z, Zheng X, Zhang H, Guo Y and Zhou B 2006 *Opt. Lett.* **31** 2789
[5] Schwelb O 2004 *J. Lightw. Technol.* **22** 1380
[6] Barwicz T, Popovi M, Watts M, Rakich P, Ippen E and Smith H 2006 *J. Lightw. Technol.* **24** 2207
[7] Xia F, Sekaric L and Vlasov Y 2007 *Nat. Photon.* **1** 65

[8] Tobing L, Dumon P, Baets R and Chin M 2008 *Opt. Lett.* **33** 2512

[9] Morichetti F, Canciamilla A, Torregiani M, Ferrari C, Melloni A and Martinelli M 2010 *SPIE* **77** 1913

[10] Heebner J, Chak P, Pereira S, Sipe J and Boyd R 2004 *J. Opt. Soc. Am.* B **21** 1818

[11] Landobasa Y, Darmawan S and Chin M 2005 *IEEE J. Quantum Electron.* **41** 1410

[12] Hu Y T, Xiao X, Zhu Y, Xu H H, Zhou L, Fan Z C, Li Y T, Li Z Y, Yu Y D and Yu J Z 2010 *IEEE 7th Int. Conf. on Group IV Photonics* Beijing September 1–3, 2010 p. 216

[13] Zhu Y, Xu X J, Li Z Y, Zhou L, Han W H, Fan Z C, Yu Y D and Yu J Z 2010 *Chin. Phys.* B **19** 014219

[14] Huang Q Z, Yu J Z, Chen S W, Xu X J, Han W H and Fan Z C 2008 *Chin. Phys.* B **17** 2562